Jurnal Tribologi 30 (2021) 61-72

MYTRIBOS Malaysian Tribology Society

Jurnal Tribologi

Website : jurnaltribologi.mytribos.org e-issn: 2289-7232

Crystallinity and cell viability in plasma-sprayed hydroxyapatite coatings

Sachin Ganeshrao Solanke [1], Vivek Gaval [1*], Amit Pratap [2], Manish Pasarkar [3]

[1] Department of General Engineering, Institute of Chemical Technology, 400019 Mumbai, INDIA.
[2] Department of Oils, Oleochemicals and Surfactants Technology, Institute of Chemical Technology, 400019 Mumbai, INDIA.
[3] Department of Mechanical Engineering, Bajaj Institute of Technology, 442001 Maharashtra, INDIA.
[*]Corresponding author: vr.gaval@ictmumbai.edu.in

KEYWORDS

Plasma-spray technique
Standoff distance
Microstructure
Crystallinity
Cell viability

ABSTRACT

Poor crystallinity of HA coating accelerates the rate of bioresorption leading to poor adhesion between coating and substrate. This is due to rapid mass loss of HA coatings resulting in poor stability and hence loosening of implants. Therefore, in the present work an attempt is made to improve crystallinity of HA coating using plasma spraying process. To achieve this HA coatings were developed on titanium Grade 2 substrates at various standoff distances in the plasma spraying process. All the HA-coated substrates were characterized using X-ray diffraction and scanning electron microscopy to analyze the phase and microstructure of the HA coatings. The results demonstrate formation a highly crystalline (~90%) and desirable dense bio-active hydroxyapatite coating on the substrate at a standoff distance of 230 mm. In addition to this cell viability test was also carried out on all HA coatings to study cells survival and interaction with coated material.

1.0 INTRODUCTION

Hydroxyapatite [$Ca_{10}(PO_4)_6(OH)_2$] is a clinically established and accepted bioceramic with the same chemical composition as human bones. In the last decades, it has been widely employed in the biomedical field for orthopedic load-bearing implants. Hydroxyapatite is commonly used to

Received 27 June 2021; received in revised form 10 July 2021; accepted 20 August 2021.
To cite this article: Solanke et al. (2021). Crystallinity and cell viability in plasma-sprayed hydroxyapatite coatings. Jurnal Tribologi 30, pp.61-72.

cover medical metallic implants (Khanal et al., 2014). Non-cemented metallic prostheses are commonly used for younger patients in today's market. This prosthesis has a bioceramic coating, such as hydroxyapatite powder. In comparison to cemented prostheses, non-cemented metallic prostheses are more stable. Early failure or deterioration of cement in cemented metallic prosthesis leads to inadequate stability, resulting in implant loosening (Paital & Dahotre, 2009; Chevalier & Gremillard, 2009). In cemented prostheses, the degradation and cracking of cement after some years are observed due to everyday human limb movements and variations in the mechanical characteristics of the femoral stem and bone cement. Implants fail as a result of cement degradation and cracking (Capitanu et al., 2018). It has also been documented in the published literature that unfavorable oxyhydroxyapatite, tri-calcium phosphate (TCP), tetra-calcium phosphate (TTCP), and calcium oxide (CaO) phases occur in HA coating when using the thermal spray approach due to improper process parameter selection (Roy et al., 2018). These phases are soluble in bodily fluids and might induce implant instability (Saini et al., 2015). The generation of these phases can be reduced by carefully selecting process parameters during the plasma HA coating process. By doing so, these phases are removed, residual stresses are reduced, and the crystalline structure of the HA coatings is enhanced (Parihar et al., 2018; Dey et al., 2014; Montay & Cherouat, 2004). To develop the HA-based bioimplant composites prosthetic, several fabrication procedures were thoroughly investigated. Out of this Food and Drug Administration (FDA) in the United States recommends plasma spraying because it has superior HA coating qualities than other coating processes (Sun, 2018). Because of the high melting point of HA, most techniques for fabricating HA prostheses have employed elevated temperatures. The difficulty with these strategies is controlling the dissociation of HA from other phases. HA powder is subjected to high temperatures throughout these procedures. These high temperatures cause HA to thermally decompose into new phases.

To create HA-coated prosthetics with long-term usefulness, the dissociation of HA bio-ceramic must be controlled. One of the most important requirements for bioimplant coatings is HA phase purity. Failures are mostly caused by HA powder particle disintegration, low crystallinity coatings, low purity, and weak adhesion/bonding strength between the implant and coating. Standoff distance (SOD) has been defined as a deciding parameter that primarily affects the properties of microstructures and HA coatings. Few countable studies like one or two are available on varying SOD. Stainless steel, titanium, and cobalt alloys are among the metallic materials used as synthetic orthopedic bone implants (Capitanu et al., 2018; Mohamed et al., 2019; Thounaojam & Birru, 2020). Titanium Grade 2 (TIGR2) is selected as a bare substrate in this study since it is less economical than other metallic alloys. Mechanical characteristics of TIGR2 are similar to Ti-6Al-4V alloy (Solanke et al., 2021; Solanke & Gaval, 2020a, Solanke & Gaval, 2020b). It has been reported that TIGR2 has a high potential for creating a successful surface structure that could be used in bioimplant clinical applications (Singh et al., 2020; Kiruthika et al., 2019; Rebeka et al., 2015). However, there is a scarcity of data on the crystallinity of HA-coated TIGR2 substrates and cell viability behavior when using the plasma spray technique with differing SOD levels.

There has been no systematic study into the fabrication and characterization of HA coating on TIGR2 substrate, according to a thorough review of the relevant literature. The development of a HA coating with high crystallinity and optimal porosity (dense and flatten structure) at varying SOD on TIGR2 substrates is reported in this communication. The scope of the problem and the objective of the present research have been formulated after a detailed literature review. Detailed investigations are required to be carried out to achieve quality HA-coated TIGR2 material bio-

implants. The goal of this research was to increase coating crystallinity and analyze the relationship between crystallinity, coating microstructure, and SOD.

2.0 EXPERIMENTAL PROCEDURE

2.1 Plasma HA-Coating Preparation

The HA coating on TIGR2 using plasma spray technique was carried out at Plasma Biotal India Ltd., Pune, India. The TIGR2 substrates were obtained in solid form having 40 mm diameter and 4 mm thickness. The sintered and granulated HA powder having crystallinity > 95%, Phase purity > 95% and Ca/P ratio- 1.67 was used as a feedstock. HA meets the requirements of the ISO 13779-6 international standard (ISO 13779-6). Prior to HA coating on metallic substrates, the metallic samples were grit blasted at 4-5 bar blasting pressure to strengthen the bond between the HA coating and the metallic sample. The presence of contaminants or dirt on the surface of the metallic substrate weakens the bond strength of the coating, resulting in delamination or cracking. The ultrasonic cleaning was carried out for 5 minutes to remove alumina grit particles which got embedded on metallic substrate during blasting. The preparation of coating was done as per ISO 19227:2018 standard (ISO 19227). Table 1 presents the plasma spray technique process parameters used for coating of HA powder on TIGR2 substrates. Argon was selected as both the primary and secondary gas in this investigation to prevent oxidation. Secondary gas creates an inert shroud over the particles that shields against the oxidation of HA.

Table 1 Plasma process parameters to develop HA coatings.

Parameters	Unit	Values
Plasma power	kW	25- 28
Primary and secondary gas	-	Argon
Standoff distance (SOD)	mm	230, 280
Flow rate	g/min	8-10
Traverse Velocity	mm/s	38-46

2.2 Microstructure Characterization of HA Coating

The HA sprayed coatings were examined under FE-SEM (ZEISS- Gemini, Cambridge CB 1 3JS, United Kingdom) for microstructure characterization of the HA coatings at MMMF lab, IIT Bombay. The EMPYREAN spectrometer equipment was utilized to perform XRD analysis in order to determine the phase composition of plasma HA powder as well as plasma HA coatings on TIGR2. During X-ray diffraction the 2θ value was kept between 20° to 80° with 0.02° step size. Double-sided tape was used to secure the coated HA metallic substrates to the XRD plate. The percent (%) crystallinity is then determined using equation 1 (Tsui et al., 1998; Sun et al., 2003).

$$\%\ Crystallinity = \frac{\sum Ac}{\sum Ac + \sum Aa} \times 100 \qquad (1)$$

Where ΣAc is the sum of the areas of all HA crystalline peaks and ΣAa is the sum of the area under the amorphous peak. Only HAP peaks were observed in the HA coating's XRD patterns (Figure 1). In terms of peak intensity and location, it is obvious there is a perfect match with the standard (JCPDS file no: 09-0432).

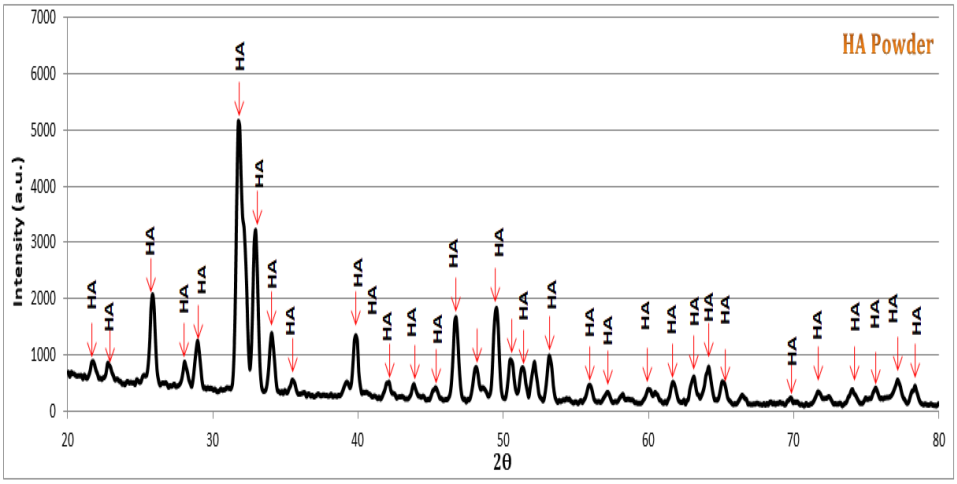

Figure 1: XRD pattern of HA powder.

2.3 Microhardness of The Coating

The nanoindentation technique was used to evaluate two local mechanical properties: micro-hardness (H) and elastic modulus (E). Nanoindentation test was carried out at industrial research and consultancy center, IITB (Hysitron Inc Minneapolis USA, TI-900). Ten indents were made for each coated sample at different location on the sample. Ten repeat experiments were performed on each HA coated samples and average value of ten tests was considered. For the nanoindentation experiments Berkovich indenter was used with 65.3^0 semi-apex angle and small tip radius around ~200 nm. The nanoindentation experiments were carried out using DIN 50359-1 standard.

2.4 Cell Viability/Culture Study

Osteoblast cells were cultured on the HA-coated samples at 230 and 280 mm SOD. The cells were grown in Dulbecco's Modified Eagle Medium (DMEM) low glucose supplement with 10% fetal bovine serum at 37°C in a humidified atmosphere containing 95% air and 5% CO_2 (FBS). The plasma-sprayed HA-coated surfaces were washed three times with a fresh medium before being washed with 95% ethanol oil. Autoclaving at 100-120 ^{0}C for 15-30 minutes sterilized all of the samples. The morphology of the cells on the HA-coated samples was analyzed using fluorescence microscopy images after 10 days of incubation.

3.0 RESULTS AND DISCUSSION

Figures 2(a) and 2(b) show photographs of an uncoated metal substrate before coating and an HA-coated sample after plasma spray coating.

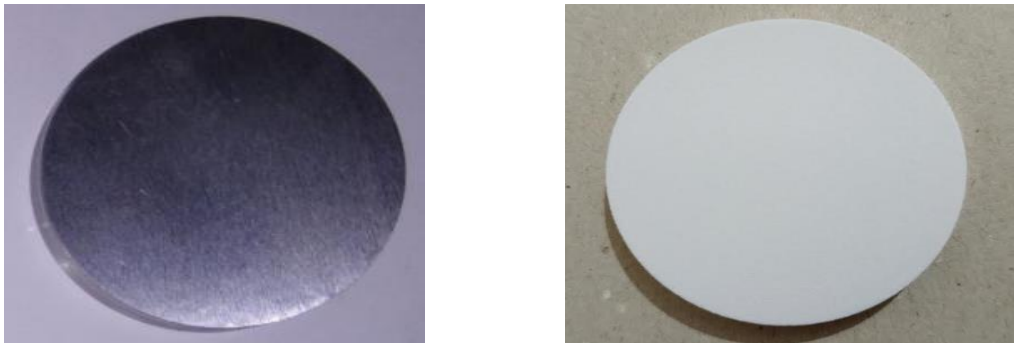

(a) (b)

Figure 2: Photograph of (a) uncoated metallic samples and (b) HA-coated sample.

Figure 3 shows the plan-sectional microstructures of the plasma-sprayed HA coatings developed at a SOD of 230 mm and 280 mm, respectively. A deeper SEM examination showed that at 280 mm SOD, the HA coating contains various cavities and macropores, which can be due to the HA particle impingement velocity on the substrate. Some HA particles might be unable to reach the end of the sample due to the journey of long-distance and reduction in velocity of an HA particle. The particles could solidify partially before reaching to the substrate samples due to the long distance and the drop in plume temperature which in turn produces splats which are randomly deposited leading to form further micro-pores structure and as observed and also reported in published research. (Sarikaya, 2005; Lu et al., 2002; Shilpa et al., 2021). Figures 3(e-f) i.e. coating at 230 mm SOD show a structure with flattened splats (much denser structure) and fewer voids, indicating increased layer packing, which eliminates the inter-splat area and particle melting, resulting in a standard lamellar structure with splat bonding. This might be because the in-flight particles have a higher velocity at 230 mm SOD. Table 2 shows microstructural properties of plasma-sprayed HA coatings developed at different 230 and 280 mm.

3.1 Plasma-Sprayed HA Coatings Phase Identification

Figures 4 and 5 show the XRD spectra of HA powder and plasma-sprayed HA coatings produced at 230 and 280 mm SOD. XRD pattern of the HA coating obtained at 230 mm SOD was found to be like XRD traces of HA powder. Whereas XRD pattern of the HA coating formed at 280 mm SOD shows the increased and shrunk peaks at different 2 theta values. At 280 mm SOD, this might be due to the thermal disintegration (thermodynamic phase change) of HA particles. At 31.86°, a major HA intensity peak appears in the powder as well as in HA coating fabricated at 230 and 280 mm SOD. In HA coatings, the diffraction pattern clearly shows the development of more amounts of additional phases such as TTCP, TCP, and CaO from peak positions of 29.45° to 33.35° and some minor at different 2 theta positions.

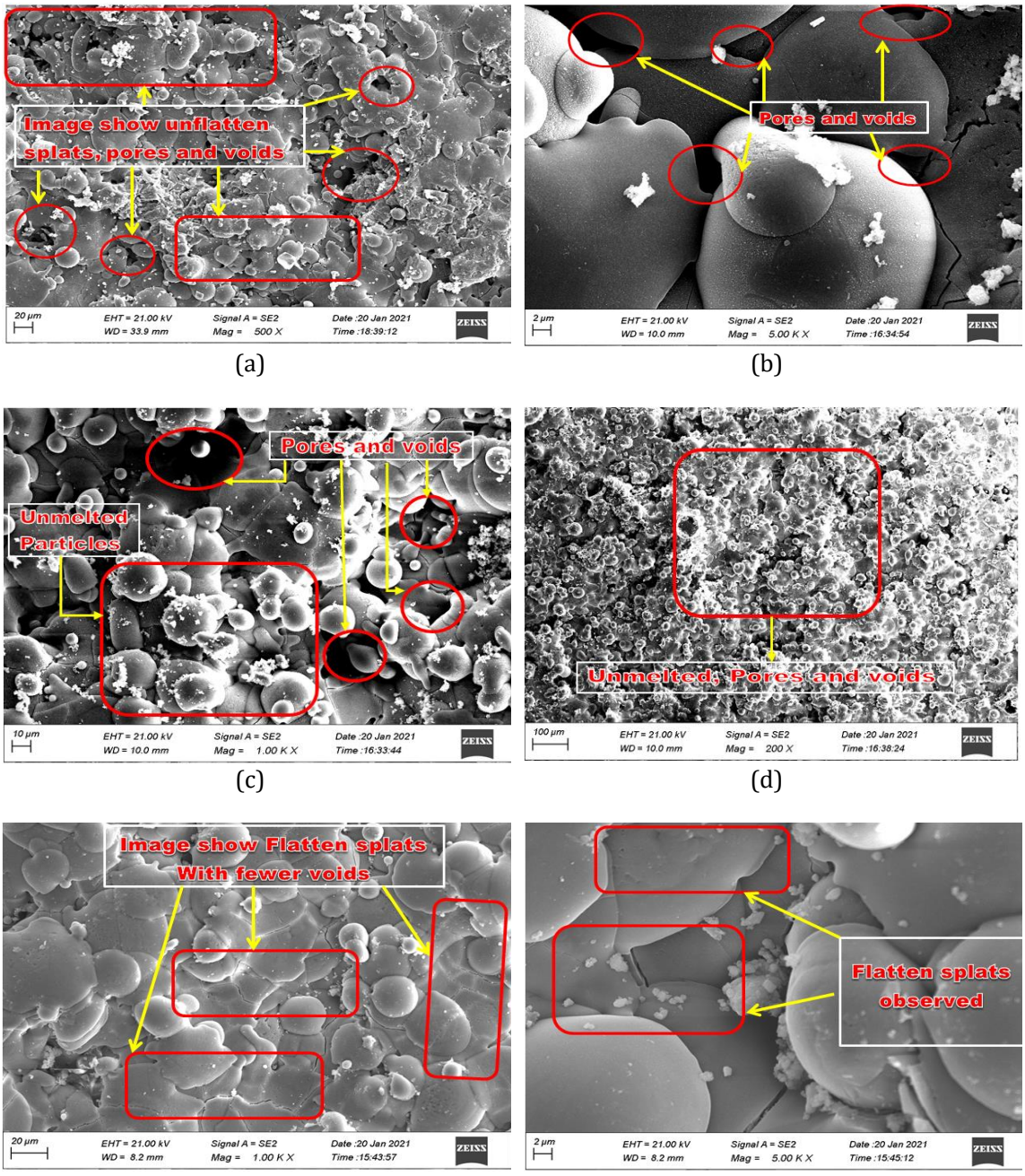

(a) (b)

(c) (d)

(e) (f)

Figure 3: Micrographs of plasma coatings on TIGR2 at 280 (a-b-c-d) and 230 (e-f) mm SOD.

Table 2: Microhardness properties of the HA coating at 230 and 280 mm SOD.

Plasma sprayed HA coatings	Microhardness of the coating (GPa)	Elastic modulus of coating (GPa)
SOD: 230 mm	2.9±0.70	86±1.07
SOD: 280 mm	2.1±0.85	71±1.15

The intensities of the amorphous calcium phosphate phases have risen with increasing SOD, which might be attributable to an increase in residence time in the plasma flame. A more degree of phase transformation occurs as HA particles spend more time in the plasma flame. The presence of TTCP, TCP, and CaO phases, according to literature, has a negative effect on the coating's crystallinity. Equation 1 has been used to calculate the crystallinity percent of plasma-sprayed HA coatings for lower and higher SOD.

At 230 mm SOD, the crystallinity ratio was ~90%, and at 280 mm SOD, it was ~76%. Thus, increasing the SOD from 230 to 280 mm SOD resulted in a ~19% decrease in crystallinity. This may be attributed to the increased amorphous phases such as TTCP, TCP, and CaO phases in the plasma sprayed HA coatings. As stated earlier, a decrease in crystallinity speeds up the HA coating's disintegration in the vivo environment. In vivo dissolution is undesired because it results in a weaker coating that is unable to protect the implant in the long term, leading to implant failure. As a result, a greater SOD level reduces crystallinity. Also, a higher 280 mm SOD raises the pores in the HA structure, potentially lowering the coating's fracturing power.

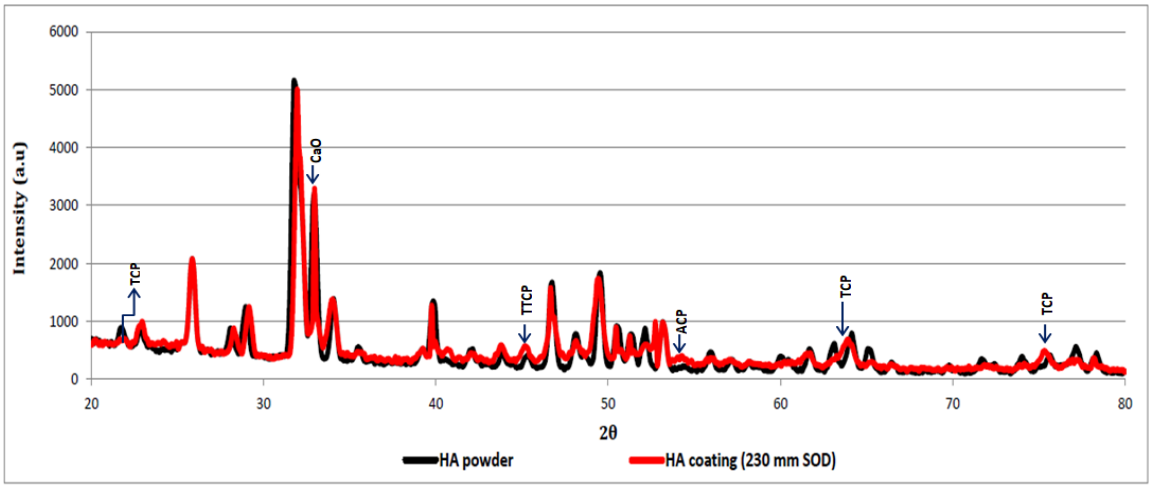

Figure 4: Comparison of XRD pattern between HA powder and HA coating (230 mm SOD).

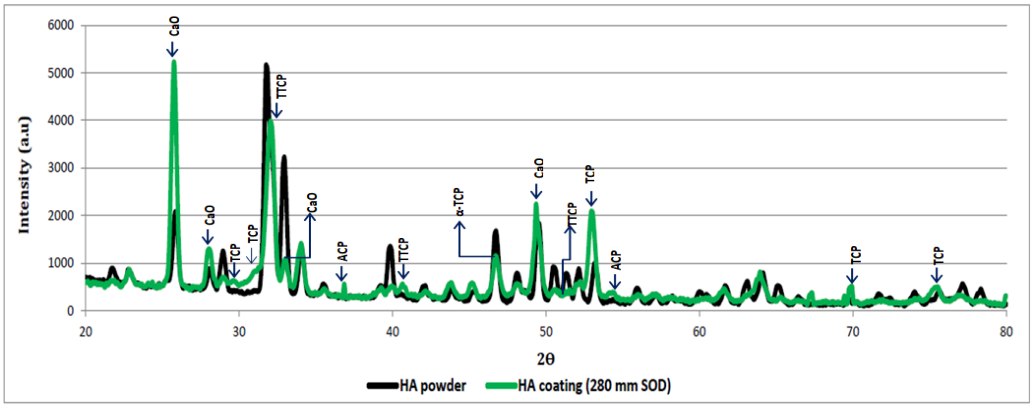

Figure 5: Comparison of XRD pattern between HA powder and HA coating (280 mm SOD).

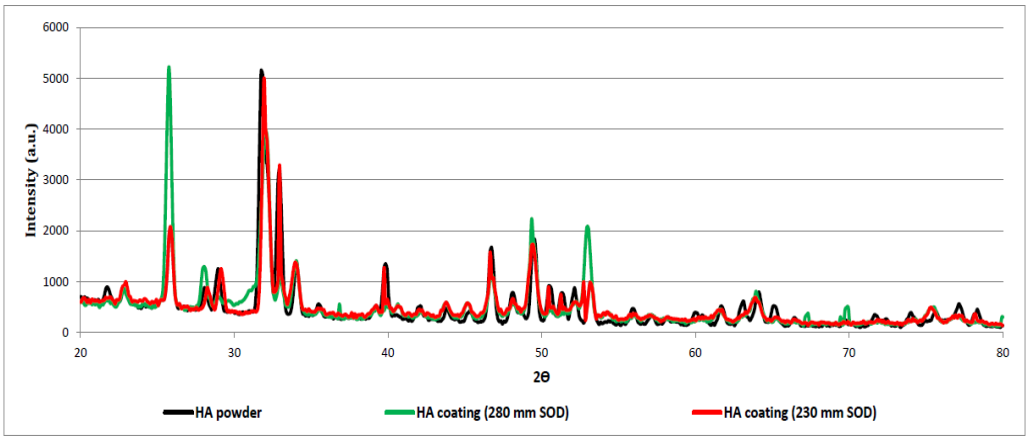

Figure 6: Comparison of XRD pattern between HA powder and HA coating (230 & 280 mm SOD).

The current HA coating fabricated by varying SOD had a higher hardness and crystallinity value than the commonly reported hardness and crystallinity values for microplasma sprayed or high velocity oxy-fuel sprayed HA coatings (Fomin et al., 2018; Dey & Mukhopadhyay, 2015). Whereas the HA coating deposition methods microstructure characterization of HA coating used in the present research are not similar to those used in the literature, a direct comparison of the present experimental data with the reported literature data was not possible in the strictest sense of the term and was therefore avoided. Figure 7 shows the % crystallinity of coatings at 230 and 280 mm SOD.

3.2 Cell Viability Analysis

This study focused on the viability of osteoblast cells on a HA-coated surface at 230 and 280 mm SOD. The quantitative ratio of live to dead cells is used to determine the viability of osteoblast cells. All counts were done in triplicate, with the sum of the three counts taken. After 10 days of growth, the fluorescence images in figure 8 (a, b, c, d) show live cells in green and dead cells in red on a HA-coated surfaces. On both surfaces i.e., HA coating at 230 and 280 mm SOD, the population of osteoblasts grows visibly from 1 to 10 days. The cell population increased dramatically after

10 days of development, completely covering the coating surface. The percentages ratio of dead and live cells for HA surfaces fabricated at 230 mm and 280 mm SOD was found to be comparable with marginal difference, meaning that they behave similarly in terms of osteoblast viability.

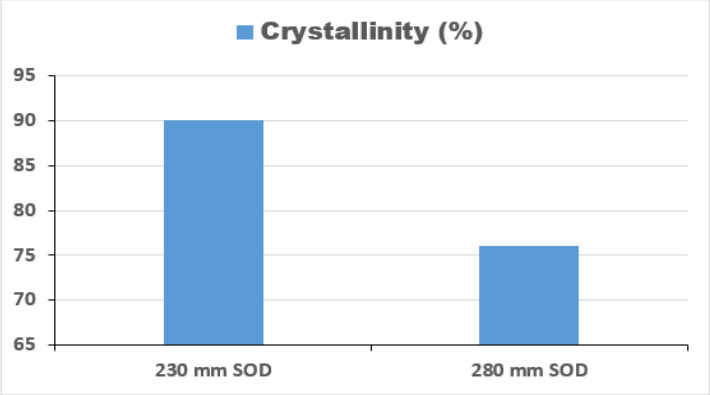

Figure 7: % crystallinity of coatings at 230 and 280 mm SOD.

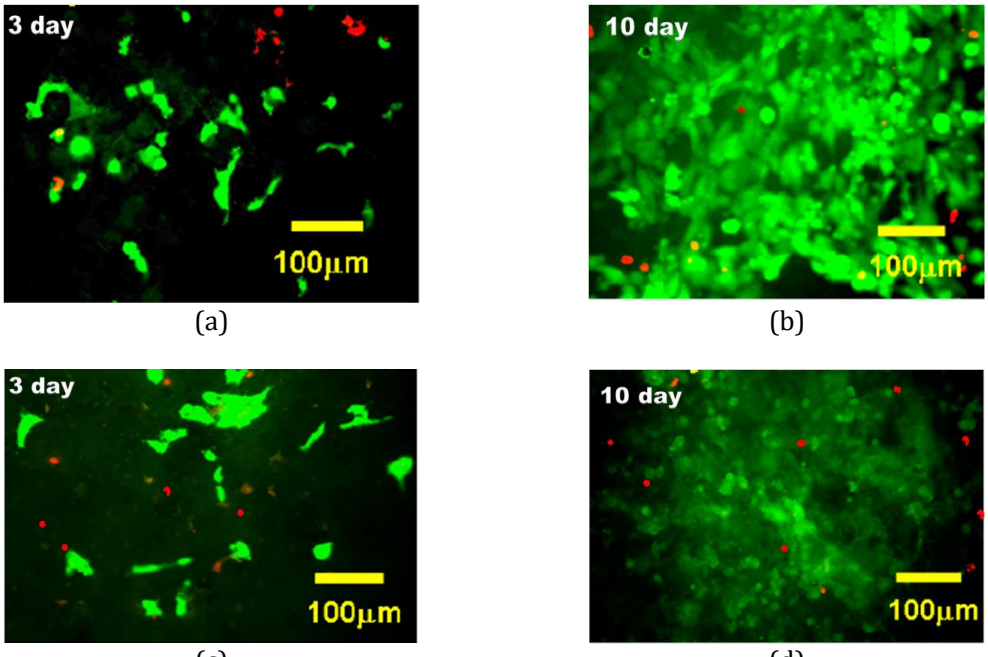

Figure 8: Fluorescent images of osteoblast cells grown for 10 days on (a-b) HA coating at 230 and (c-d) 280 mm SOD.

Cell viability on the HA-coated sample was ~92% and ~84% at 230 and 280 mm SOD respectively, as seen in figure 9. This marginal variation may be due to the partial dissolution of amorphous calcium phosphate phases due to the non-crystalline HA composition of coatings and

the surrounding solution's concentration. Figure 9 shows the % viability of cells for 10 days at 230 and 280 mm SOD.

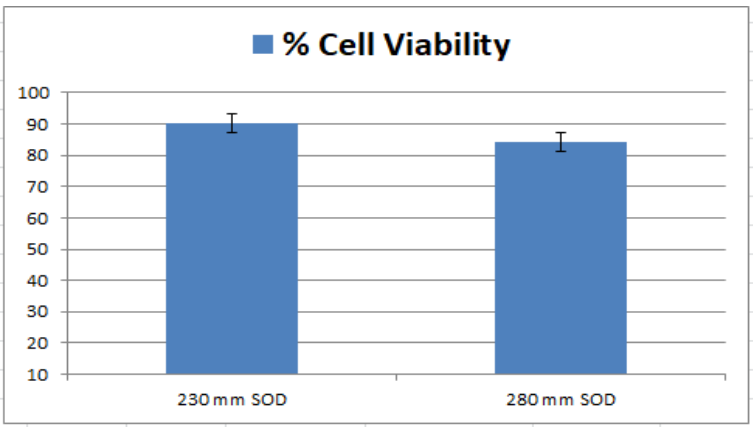

Figure 9: Viability of cells for 10 days.

4.0 CONCLUSION

Longer residence time in the plasma flame at 280 mm SOD results in more heat work on the powder and a greater quenching amount upon 'splat' due to additional work which leads to the formation of the weak coating. On other hand, optimal pores with flatten splats, denser structure, and fewer voids were observed at 230 mm SOD as compared to higher 280 mm SOD, which is attributed to higher HA particle velocity due to optimal SOD. This increased the flattening ratio of the spreading splats. XRD results showed that HA coating at 230 mm SOD had a better crystalline structure. Cell viability was found to be marginally better at 230 mm SOD as compared to the HA-coated TIGR2 sample at 280 mm SOD. This could be due to the large number of dead cells observed at 280 mm SOD during the time being. Therefore, HA coating fabricated at 230 mm SOD can be considered as better rather than at 280 mm SOD.

ACKNOWLEDGMENTS

The authors sincerely thank to Plasma Biotal India Pvt. Ltd., Pune, India for providing the HA coatings and testing facility and support. The authors are thankful to MMMF Lab, IIT-B, Mumbai, INDIA for providing the experimental facilities like XRD, SEM etc. I am equally thankful to NFST, New Delhi, India for providing financial support during research work.

REFERENCES

Capitanu, L., Badita L., & Florescu, V. (2018). Initiation of fretting fatigue scar of Ti-6Al-4V alloy dependent on the influence of its surface roughness. Jurnal Tribologi, 19, 19-38.

Capitanu, L., Badita, L., & Florescu V. (2018). Investigation a unique scratching of the failure mechanisms of the coatings with TiN thin layers deposited on 316L stainless steel. Jurnal Tribologi, 17, 40-64.

Chevalier, J., & Gremillard, L. (2009). Ceramics for Medical Applications: A Picture for the next 20 Years. Journal of Eur. Ceramic Society. 29, 1245–1255.

Dey, A., & Mukhopadhyay, A. K. (2015). Nanoindentation Study of Phase-pure Highly Crystalline Hydroxyapatite Coatings Deposited by Microplasma Spraying. Open Biomed Eng Journal, 9, 65-74.

Dey, A., Sinha, A., Banerjee, K., & Mukhopadhyay, A. K. (2014). Tribological studies of microplasma sprayed hydroxyapatite coating at low load. Materials Technology, 29, 35-40.

Fomin, A., Fomina, M., Koshuro, V., Rodionov, I., Zakharevich, A., & Skaptsov, A. (2017). Structure and mechanical properties of hydroxyapatite coatings produced on titanium using plasma spraying with induction preheating, Ceramics International, 43 (14), 11189-11196.

ISO 13779-6, Implants for surgery Hydroxyapatite- Part 6: Powders, 2015.

ISO 19227, Implants for surgery-Cleanliness of orthopedic implants-General requirements, 2018.

Khanal, S. P., Mahfuz, H., Rondinone, A. J., & Leventouri, T. (2016), Improvement of the fracture toughness of hydroxyapatite (HAp) by incorporation of carboxyl functionalized single walled carbon nanotubes (CfSWCNTs) and nylon. Mater Sci Eng C Mater Biol Appl. 60, 204-210.

Kiruthika, L., Huirong, L., Christopher, T., & Richard, D. H. (2019). Carbon Nanotube Reinforced Hydroxyapatite Nanocomposites As Bone Implants: Nanostructure, Mechanical Strength And Biocompatibility. International J Nanomedicine, 14, 7947-7962.

Lu, Y., Li, S. T., Zhu, R. F., & Li, M. S. (2002). Further studies on the effect of standoff distance on characteristics of plasma sprayed hydroxyapatite coating Surface and Coatings Technology, 157 (2), 221–225.

Mohamed, R., Ghani, S. A. C., & Sawangsri, W. (2019). Mechanical properties of additive manufactured CoCrMo meta-biomaterials for load bearing implants. Jurnal Tribologi, 21, 93-107.

Montay, G., & Cherouat, A. (2004). Residual stresses in coating technology. Journal of Materials Science and Technology-Shenyang, 20, 81-84.

Paital, S., & Dahotre, N. (2009). Calcium Phosphate Coatings for Bio-Implant Applications: Materials, Performance Factors, and Methodologies. Material Science Engineering, 66, 1–70.

Parihar, R. S., Setti, S. G., & Sahu, R. K. (2018). Recent advances in the manufacturing processes of functionally graded materials: a review. Science and Engineering of Composite Materials, 25, 309-336.

Rebeka, R., Dragoslav, S., Zoran, A., & Monika, J. (2015). HYDROXYAPATITE COATINGS ON Cp-TITANIUM GRADE-2 SURFACES PREPARED WITH PLASMA SPRAYING. Materiali in Tehnologije, 49(1), 81-86.

Roy, M., Bandyopadhyay, A., & Bose, S. (2011). Induction Plasma Sprayed Nano Hydroxyapatite Coatings on Titanium for Orthopaedic and Dental Implants. Surf Coat Technol., 205, 2785-2792.

Saini, M., Singh, Y., Arora, P., Arora, V., Jain, K., (2015). Implant biomaterials: A comprehensive review. World J Clin. Cases, 3(1), 52-57.

Sarikaya, O. (2005). Effect of some parameters on microstructure and hardness of alumina coatings prepared by the air plasma spraying process. Surf Coat Technol., 190 (2-3), 388-393.

Shilpa, C., Mahesha, K., Dey, A., & Sachidananda, K. B. (2021). Effect of standoff distance (SOD) on damping properties of atmospheric plasma sprayed alumina-zirconia ceramic coatings. surface engineering, 37 (5), 599-605.

Singh, S., Pandey, K. K., Rahman, O., Haldar, S., Debrupa, L., & Keshri A. K. (2020). Investigation of crystallinity, mechanical properties, fracture toughness and cell proliferation in plasma

sprayed graphene nano platelets reinforced hydroxyapatite coating. Materials Research Express, 7 (1).
Solanke, S. G., & Gaval, V. R. (2020a). Optimization of wet sliding wear parameters of Titanium grade 2 and grade 5 bioimplant materials for orthopedic application using Taguchi method. Journal of Metals, Materials and Minerals, 30 (3).
Solanke, S. G., & Gaval, V. R. (2020b).Tribological Studies of Different Bioimplant Materials for Orthopaedic Application. ASM Sc. J., 13, 1-8.
Solanke, S., Gaval, V., & Sanghavi, S. (2021). In vitro tribological investigation and osseointegration assessment for metallic orthopedic bioimplant materials. In Proceedings of Materials Today Conference, pp. 4173-4178.
Sun, L. (2018). Thermal Spray Coatings on Orthopedic Devices: When and How the FDA Reviews Your Coatings. J Therm Spray Tech, 27, 1280–1290.
Sun, L., Berndt, C. C., & Grey, C. P. (2003). Phase, structural and microstructural investigations of plasma sprayed hydroxyapatite coatings. Materials Science and Engineering A, 360, 70-84.
Thounaojam, A., & Birru, A. K. (2020). Bone machining: An analysis of machining parameters such as cutting speed, feed rate, and depth of cut using bovine bone. Jurnal Tribologi, 24, 39-51.
Tsui, Y. C., Doyle, C., & Clyne, T. W. (1998). Plasma sprayed hydroxyapatite coatings on titanium substrates Part 1: Mechanical properties and residual stress levels. Biomaterials, 19, 2015-2029.